JOURNAL OF MATERIALS SCIENCE **39** (2004) 565–570

Sol-gel titania modified with Ba and Li atoms for catalytic combustion

T. LÓPEZ
Deparment of Chemistry, Universidad Autónoma Metropolitana-Iztapalapa, A.P. 55-534, 09340 México D. F., México

A. HERNÁNDEZ
Facultad de Ciencias Químicas, División de Estudios Superiores, Universidad Autónoma de Nuevo León, A.P. 1625, Monterrey, Nuevo León, Mexico

X. BOKHIMI
Institute of Physics, The National University of México (UNAM), A.P. 20-364, 01000 México D. F., Mexico

L. TORRES-MARTINEZ
Facultad de Ciencias Químicas, División de Estudios Superiores, Universidad Autónoma de Nuevo León, A.P. 1625, Monterrey, Nuevo León. Mexico

A. GARCÍA
UPIICSA, COOFA, Instituto Politécnico Nacional, México D. F., Mexico

G. PECCHI*
Faculty of Chemistry, University of Concepción, P.O. Box 160-C, Concepción, Chile
E-mail: gpecchi@udec.cl

Samples of compounds in the ternary system BaO-Li_2O-TiO_2 were synthesized by using the sol-gel method at pH 3 and pH 9, and the calcination temperatures of 600 and 800°C in the region of solid solutions which can form the "ideal" composition $Ba_3Li_2Ti_8O_{20}$. The X-ray diffraction patterns of the samples showed a mixture of three crystalline phases, the main one was isostructural with the ternary phase $Ba_3Li_2Ti_8O_{20}$; the other two were $BaTiO_3$ and Li_2TiO_3. By refining the structures with the Rietveld technique, a good fit to the experimental diffraction pattern was found, showing the partial substitution of Ti by Li in the $Ba_2Ti_6O_{13}$ structure. The catalytic activity in methane combustion under the stoichiometric mixture of dilute CH_4/O_2 was higher for the samples calcined at 600°C, where the $Ba_3Li_2Ti_8O_{20}$ ternary compound was formed. This high activity can be related with the large specific surface area, presence of anatase and low crystallite size.

1. Introduction

Catalytic combustion is one of the industrial processes for pollution abatement. The catalysts able to perform combustion are divided in two groups: noble metals [1, 2] which can react at room temperature, and transition metal oxides, which are less efficient, but more resistant at high temperatures [3].

Industrial emissions are normally formed under conditions in which the catalysts are exposed at high temperatures to water vapor and sulfur compounds in the feed. It has been reported that water vapor may induce the migration of metal crystallites leading to the sintering of the active phase [4], effect that can be minimized using the sol-gel method in the catalyst preparation [5, 6].

Sol-gel mixed oxides can be modified by doping them with lithium and barium. As lithium is incorporated in the form of an ionic salt into the aqueous solution used for the synthesis, its distribution in titanium network is expected to be very homogeneous. In the case of barium, it is co-gelled as barium isopropoxide forming highly reactive ─Ba─OH species therefore the ─Ba─O─Ti─ bond should be formed in the net. As all these species are present in the initial sol; they also would be present in the gel, and therefore, finally at 800°C the $Ba_3Li_2Ti_8O_{20}$ is formed. This material has a very large numbers of applications due to its optical, chemical, mechanical and catalytic properties [13, 14].

Suckut *et al*. [15] studied the ternary phases formation in the system BaO-Li_2O-TiO_2, and its electrical properties. They found four ternary phases with variable composition; forming solid-solutions obtained by solid-state reaction at 1200°C for 10 days.

*Author to whom all correspondence should be addressed.

By using the sol-gel process it is possible to prepare these ternary systems at low temperature with a great saving of energy. Sol-gel processing in which metal organic precursors are mixed with appropriate salts, hydrolyzed through the addition of water, carefully controlling the pH and the reaction temperature. As hydrolysis and polymerization occur, colloidal particles or micelles with an approximate diameter of 10 nm are formed [16]. These particles continue to increase in size until a metal oxide gel is formed [17].

In the sol-gel method, a greater degree of control over the material preparation can be achieved in comparison with the traditional synthesis methods. The molecular compounds formed as a result of polymerization of the organic and inorganic precursors using this sol-gel synthesis approach have unusual physical and chemical properties: They form stable solids at low temperature with unusually pore structure and particles in the nanosize range.

2. Experimental

In 200 ml of ethanol (99.9% PROQUIM) 20.37 g of barium isopropoxide (Aldrich Chemicals, 99.9%) were dissolved. Separately, 5.43 g of lithium acetate (Sigma, 99.9%) were dissolved in a mixture of 48 ml of ethanol with 18.25 ml of distilled water. Ammonium hydroxide (PROQUIM 99.8%) was added to the reflux mixture under continuous stirring until pH 9 was reached. An amount of 63.28 ml of titanium isopropoxide (Aldrich Chemicals, 98%) was added to the flask containing the barium isopropoxide, before the lithium acetate solution. The final solution was stirred continuously and refluxed at 70°C until the gel was formed. The gelling time was shorter (48 h) than when samples were synthesized at pH 3 (72 h). The molar ratio $Ti[OCH(CH_3)_2]_4$/Ethanol was 1:20, while the $Ti[OCH(CH_3)_2]_4/H_2O$ was 1:10. The final product was an opaque gel of colloidal nature, which was heated slowly to 40°C for solvent evaporation. Lately the gel was dried at 90°C for 24 h (fresh sample). Before characterization, different portions of the resultant gel were annealed in air at 600° and 800°C for 6 h at each temperature. The pH 3 samples were prepared with the same procedure using HCl as hydrolysis catalyst.

3. Characterization

3.1. Raman spectroscopy

The Raman spectra of the calcined samples were recorded at room temperature in a nearly backscattering geometry using an ISA Labram micro-Raman apparatus. The excitation line was 632.8 nm of a He-Ne laser, operated at 1 mW to avoid thermal effects.

3.2. X-ray diffraction

X-ray diffraction patterns of the samples packed in a glass holder were recorded at room temperature with Cu K_α radiation in a Bruker Advance D-8 diffractometer with theta-theta configuration and a graphite secondary-beam monochromator. Diffraction intensity was measured in the 2θ range between 18 and 110°, with a 2θ step of 0.02° for 8 s per point. Crystalline structures were refined according to the Rietveld technique using DBWS-9411 code [1x]; peak profiles modeled with pseudo-Voigt functions [2x] contained average crystallite size as one of their characteristic parameters [3x]. Standard deviations, which give the last figure variation of a number, are given in parentheses; when they correspond to refined parameters, their values are not estimated to be the probable error in the analysis as a whole, but only of the minimum possible probable errors based on their normal distribution [4x].

3.3. Specific surface area

Specific surface area, pore volume and mean pore diameter were measured with an ASAP 2000 Micromeritics analyzer, via nitrogen adsorption isotherms. The specific area was calculated by the BET equation and the mean pore size diameter by the BJH method. Before measurements samples were desorbed at 300°C for 2 h.

3.4. Catalytic activity

The catalytic activity in the combustion of methane was evaluated in a conventional flow reactor operated at atmospheric pressure using 100 mg of catalysts, space velocity of 6000 h^{-1} at temperatures from 150°C up to that required for a total conversion. A heating rate of 1°C min^{-1} was used. The effluents of the reactor were analyzed by an on-line gas chromatograph. A single column containing molecular sieve (5A) was used; the chromatographic separation was carried out isothermally at 333 K with helium as carrier gas. In some experiments a quadrupole mass spectrometer Hiden HPT 20 was used to detect small traces of products.

4. Results and discussion

4.1. Raman spectroscopy

The Raman spectra of the pH 3-600°C sample had the characteristic peaks of anatase at 144, 390, 513 and 635 cm^{-1} corresponding to the active Raman modes of symmetry B1g, A1g + B1g and Eg [22, 23] are shown in Fig. 1. The low intensity peaks at 400 and 650 cm^{-1} corresponded to rutile. When the sample was annealed at 800°C, the spectra were undefined due to the $Ba_3Li_2Ti_8O_{20}$ formation. The bands of the samples calcined at 600°C were shifted from the corresponding values of the pure titanium [24] due to the presence of BaO and Li_2O. Lithium ions were diffused into the anatase channels changing the Ti─O bonds vibrations, while the nano-clusters of BaO were highly dispersed on titanium surface. In both samples calcined at 600°C, the stretching vibration assigned to O─H and ─OH were observed. The presence of the bulk hydroxyl groups changed the behavior of these solids, because they were the anchoring sites of lithium and barium ions when the temperature was increased to 800°C, forming the $Ba_3Li_2Ti_8O_{20}$ phase. On the other side, the surface hydroxyl groups, remaining stable up to 600°C inhibited the sintering of the alkaline and alkaline earth metals.

In Fig. 2 it can be seen in the 600°C-pH 9 sample, the corresponding peak of anatase at 144 cm^{-1} was broad

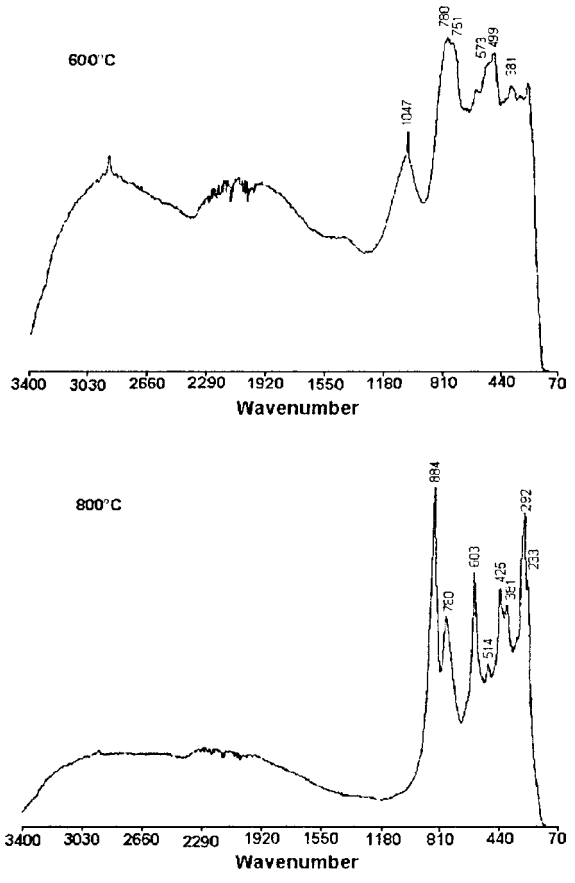

Figure 1 Raman spectra of the BaO-Li_2O-TiO_2 samples prepared at pH 3.

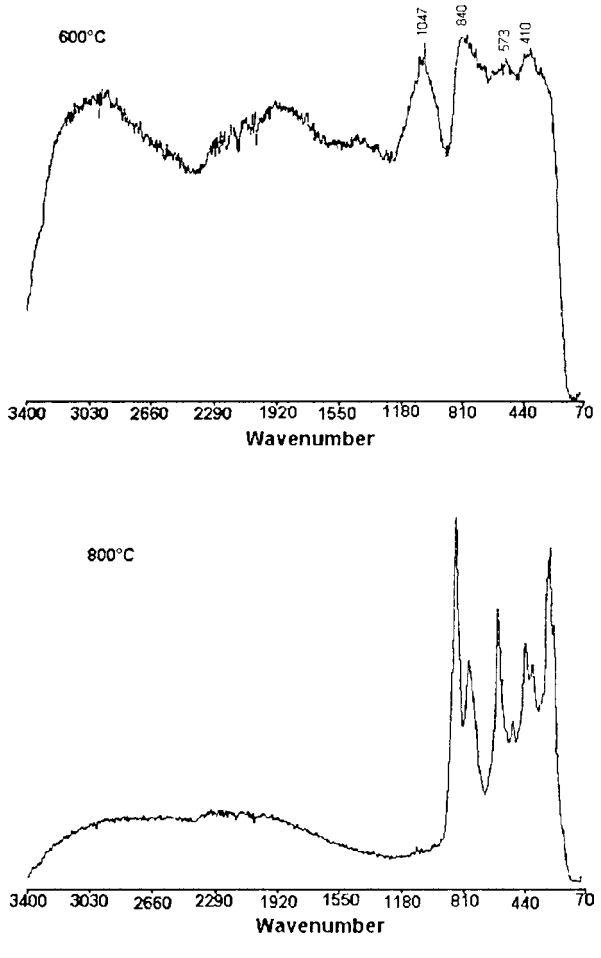

Figure 2 Raman spectra of the BaO-Li_2O-TiO_2 samples prepared at pH 9.

and shifted about 20 cm^{-1}; the finite-size effect on the phonons was not adequate to explain this broadening. The most likely origin of it was the lack of stoichiometry of the TiO_2 powders due to the presence of the hydroxyl groups. Oxygen vacancies may cause a high broadening of the Raman bands due to the long-range Coulomb interactions between the titanium and the basal oxygen atoms. The annealing in air produces only the sharpening of the peaks due to the crystal growth. The other bands remained in the same position of the 600°C-pH 3 sample.

4.2. X-ray diffraction

Figs 3 and 4 show the diffractograms of these sol-gel materials. Early studies showed that upon 600°C, the samples were amorphous and at 600°C, anatase and rutile were formed. It was shown that the presence of Ba and Li inhibited titanium crystallization at low annealing temperatures, as has been reported in other sol-gel fresh titanium systems [25, 26]. It can be seen that in the sample pH 9 calcined at 600°C the main phase was anatase; a small amount of rutile was only observed for the sample prepared at pH 3. The crystallite size of anatase in pH 9-600°C was lower than that corresponding to the pH 3-600°C sample. The stabilization

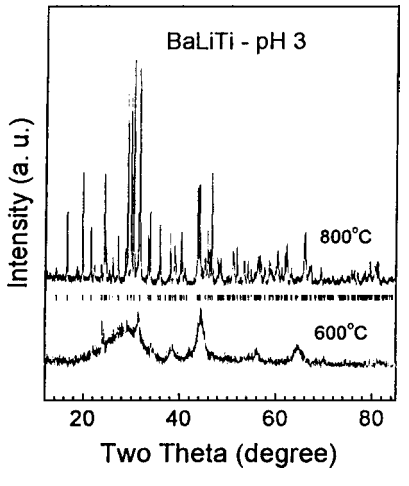

Figure 3 X-ray diffraction patterns of the BaO-Li_2O-TiO_2 samples prepared at pH 3. Tick marks correspond to anatase.

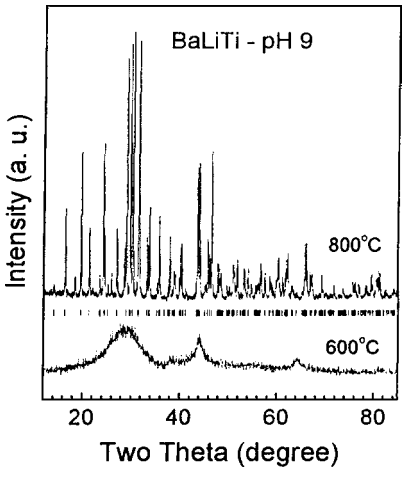

Figure 4 X-ray diffraction patterns of the BaO-Li_2O-TiO_2 samples annealed at pH 9. The tick correspond to the Li_2TiO_4 compound.

TABLE I $Ba_3Li_2Ti_8O_{20}$, pH 9, 800°C (monoclinic symmetry, space group $C2/m$): atomic fractional coordinates

Atom	Site	X	y	z	B
Ba	4*i*	0.0519(2)	0.0	0.7686(3)	1.07(8)
Ti(1)	4*i*	0.3797(5)	0.0	0.9071(7)	0.2(3)
Ti(2)	4*i*	0.2592(7)	0.0	0.231(1)	1.4(3)
Li	4*i*	0.2592(7)	0.0	0.231(1)	1.4(3)
Ti(3)	4*i*	0.3304(5)	0.0	0.5615(8)	0.5(3)
O(1)	4*i*	0.133(1)	0.0	0.123(2)	0.5(8)
O(2)	4*i*	0.264(1)	0.0	0.766(2)	1.4(7)
O(3)	4*i*	0.204(1)	0.0	0.446(2)	1.3(7)
O(4)	4*i*	0.334(1)	0.0	0.088(3)	2.5(6)
O(5)	4*i*	0.388(2)	0.0	0.409(3)	5(1)
O(6)	4*i*	0.428(2)	0.0	0.693(2)	2.1(8)

TABLE II $Ba_3Li_2Ti_8O_{20}$, pH 3, 800°C (monoclinic symmetry, space group $C2/m$): atomic fractional coordinates and thermal factors

Atom	Site	X	y	z	B
Ba	4*i*	0.0516(3)	0.0	0.7708(4)	0.7(1)
Ti(1)	4*i*	0.3786(7)	0.0	0.907(1)	0.2(4)
Ti(2)	4*i*	0.2604(8)	0.0	0.225(1)	1.7(4)
Li	4*i*	0.2604(8)	0.0	0.225(1)	1.7(4)
Ti(3)	4*i*	0.3306(7)	0.0	0.560(1)	1.2(7)
O(1)	4*i*	0.134(2)	0.0	0.123(3)	–
O(2)	4*i*	0.258(2)	0.0	0.767(2)	0.0
O(3)	4*i*	0.211(2)	0.0	0.453(3)	1.1(7)
O(4)	4*i*	0.335(1)	0.0	0.090(3)	0.0
O(5)	4*i*	0.408(3)	0.0	0.434(5)	6(2)
O(6)	4*i*	0.424(3)	0.0	0.691(4)	1.8(2)
O(7)	2*b*	0.5	0.0	1.0	1.4(2)

of anatase phase by the surface hydroxyl groups has been previously reported [27]. When the temperature was increased, the structure of the solid remained as anatase until it was transformed into the crystalline structure of $Ba_3Li_2Ti_8O_{20}$. This behavior is because at 800°C, the $Ba_3Li_2Ti_8O_{20}$ compound needs less energy to be formed, i.e., it is thermodynamically more stable than anatase or rutile. To refine the crystalline structure of this phase, it was modeled with a monoclinic unit cell that had the symmetry given by space group $C2/m$; $BaTiO_3$ was modeled with a tetragonal unit cell and the space group *P4mm*, and Li_2TiO_3, with a monoclinic unit cell and the space group $C2/c$. The diffraction patterns obtained with the above models fitted well with the experimental patterns. The initial values for the refinable parameters for the ternary phase were taken from reference [28], where it is supposed the partial substitution of Ti by Li in the $Ba_2Ti_6O_{13}$ structure.

Concerning the ternary phase, $Ba_3Li_2Ti_8O_{20}$ the refined fractional atomic positions and the refined thermal atomic factors are reported in Tables I–V. The cell parameters are also reported, as well as the average size of the crystallites which were calculated from the corresponding refined parameter, for both pH 3 and pH 9 and for the two treatment temperatures (600 and 800°C).

The concentration of each phase present in the samples, which were calculated from the refinements of the samples annealed at 800°C for both pH values, are reported in Table VI. Comparison of the patterns at 600 and 800°C, for both pH values, affirms that in the samples at 600°C a long range ordering is already present with the same crystalline structure obtained when samples were annealed at 800°C, one of the compound $Ba_3Li_2Ti_8O_{20}$, since there is a correspondence between the positions of the wide peaks of the sample pattern annealed at 600°C and the more sharp reflections observed in the sample pattern annealed at 800°C. This fact shows the presence of nanometric size crystallites at 600°C.

4.3. Specific surface area

Table VII shows the specific surface areas obtained from nitrogen adsorption isotherms at 77 K, and the mean pore diameter of the solids. The specific surface area in the samples calcined at 800°C dropped significantly indicating the crystalline solid solution formation. No effect of the gelation pH on the development of porosity in the solids was observed. The highest surface area was 49 $m^2\ g^{-1}$ for the sample prepared at pH 9 calcined at 600°C and the lowest one of 6 $m^2\ g^{-1}$ corresponding to the pH 3 sample calcined at 800°C. As a reference, TiO_2-Degussa ($S_{BET} = 72\ m^2\ g^{-1}$) was used for comparison the catalytic activity.

It is well known that when gelation of titanium alkoxide is carried out in the presence of additives, the electronegativity of the central atom is affected, which is determinant on the reactivity of the sample, for this case barium and lithium ions. If the pH is acid, we will have a nucleophilic substitution mechanism, whereas at basic pH, the hydrolysis mechanism is an electrophilic substitution; this means that a different texture and structure of the solid are obtained. In the case of the BaO-Li_2O-TiO_2 system calcined at 600°C, the materials were mesoporous for the two gelation pH values indicating no effect of the gelation pH. In the samples calcined at 800°C, the network was contracted, and the atoms rearranged to form $Ba_3Li_2Ti_8O_{20}$ without specific surface area and porosity.

4.4. Catalytic activity

The activities for methane oxidation under stoichiometric conditions (CH_4:$O_2 = 1:2$ molar) were measured as a function of the temperature up to complete combustion. The results are shown in Fig. 5, where typical sigmoidal curves were obtained in which the reaction starts

TABLE III $Ba_3Li_2Ti_8O_{20}$ (monoclinic symmetry, space group $C2/m$): lattice parameters and average crystallite size

	T (°C)	A (nm)	b (nm)	c (nm)	β (°)	d (nm)
$Ba_3Li_2Ti_8O_{20}$, pH 9	800	1.51614(4)	0.38962(1)	0.91027(2)	98.666(2)	141(7)
$Ba_3Li_2Ti_8O_{20}$, pH 9	600	1.453(4)	0.397(1)	0.851(2)	98.8450(2)	2.7(2)
$Ba_3Li_2Ti_8O_{20}$, pH 3	800	1.51647(6)	0.38955(1)	0.91034(3)	98.694(3)	110(7)
$Ba_3Li_2Ti_8O_{20}$, pH 3	600	1.599(5)	0.406(1)	0.862(4)	101.8(3)	2.8(3)

TABLE IV $BaTiO_3$ (Tetragonal symmetry, space group *P4mm*): atomic fractional coordinates

Atom	Site	*x*	*y*	*Z*
Ba	1*a*	0.0	0.0	0.0
Ti	1*b*	0.5	0.5	0.512
O(1)	1*b*	0.5	0.5	0.023
O(2)	2*c*	0.5	0.0	0.486

Lattice parameters: $a = 4.0007(3)$, $c = 4.027(5)$.

TABLE V Li_2TiO_3 (monoclinic symmetry, space group $C2/c$): atomic fractional coordinates

Atom	Site	*X*	*y*	*Z*
Li(1)	4*d*	0.25	0.25	0.5
Li(2)	4*e*	0.0	0.045	0.25
Li(3)	8*f*	0.238	0.077	0.0
Ti(1)	4*e*	0.0	0.415	0.25
Ti(2)	4*e*	0.0	0.747	0.25
O(1)	8*f*	0.141	0.265	0.138
O(2)	8*f*	0.102	0.586	0.138
O(3)	8*f*	0.138	0.906	0.135

Lattice parameters: $a = 5.077(4)$, $b = 8.759(7)$, $c = 9.765(5)$, $\beta = 100.29(7)$.

TABLE VI Phase concentration as a function of pH for the $Ba_3Li_2Ti_8O_{20}$ samples calcined at 800°C

PH	$Ba_3Li_2Ti_8O_{20}$ (wt%)	$BaTiO_3$ (wt%)	Li_2TiO_3 (wt%)
3	91(4)	5.7(2)	3.1(3)
9	95(5)	2.0(1)	3.1(2)

TABLE VII Specific surface area, mean pore diameter and catalytic activity in methane combustion expressed as ignition temperature (Ti^{50})

Catalyst	S_{BET} ($m^2\ g^{-1}$)	Mean pore diameter (nm)	T_i^{50} (°C)
BaO-Li_2O-TiO_2,3 600°C	38	24	650
BaO-Li_2O-TiO_2,9 600°C	49	–	576
$Ba_3Li_2Ti_8O_{20}$,3 800°C	6	9.3	762
$Ba_3Li_2Ti_8O_{20}$,9 800°C	9	7.6	764
TiO_2, Degussa P-25	72	4.5	752

at 450°C, then the conversion increased drastically as the temperature increased and a complete conversion was reached. Carbon dioxide and water were the main products of the reaction. However, at high conversion levels (>60%) traces of CO were also detected.

For the samples calcined at 600°C, the reaction started at lower temperature than for the corresponding ones calcined at 800°C; the activity of the samples calcined at 800°C was extremely low.

The ignition temperatures (Ti^{50}), defined as the temperature required to obtain 50% of CH_4 conversion, are compiled in Table VII. Significant differences due to the structure of the ternary oxide can be observed. The high activity at 600°C is explained due to the presence of anatase, rutile and nanocrystalline oxides of Ba and Li, meanwhile, at 800°C $Ba_3Li_2Ti_8O_{20}$ show a lower catalytic activity. The high activity of the material prepared at pH 9-600°C can be explained considering the high surface area, high extent of anatase and low crystallite size of this phase. The fact that TiO_2, Degussa displayed a high ignition temperature, i.e., low catalytic activity, than both BaO-Li_2O-TiO_2 ternary oxides calcined at 600°C, even though titanium Degussa has high surface area, is indicative that the active phase for this reaction are barium and lithium oxides.

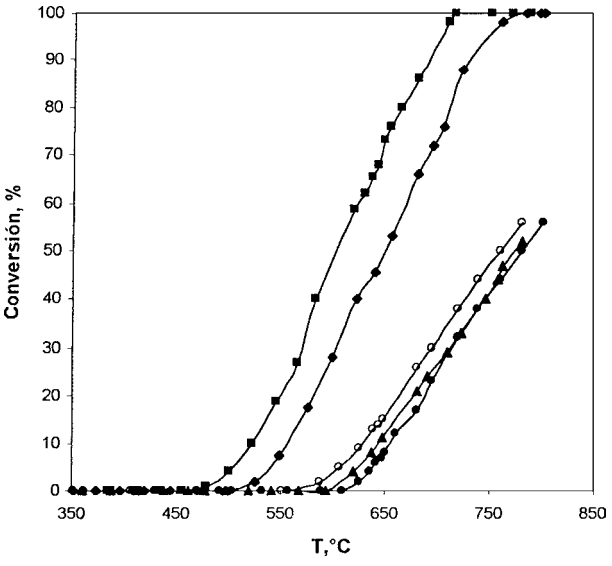

Figure 5 Catalytic activity under stoichiometric conditions in the combustion of methane for the prepared catalysts: (○) TiO_2 Degussa, (♦) BaO-Li_2O-TiO_2,3 600°C, (■)BaO-Li_2O-TiO_2,9 600°C, (▲)$Ba_3Li_2Ti_8O_{20}$,3 800°C, and (■) $Ba_3Li_2Ti_8O_{20}$,9 800°C.

5. Conclusions

By using the sol-gel method, $Ba_3Li_2Ti_8O_{20}$ can be formed at lower temperature than by solid state reaction. This compound was formed at 800°C with high crystallinity. Anatase phase can be stabilized by the hydroxyl groups present in the sol-gel material; the crystallite size in the pH 9-600°C sample was lower than for the pH 3-600°C sample.

In the BaO-Li_2O-TiO_2 system, the presence of barium and lithium inhibited the crystallization of titanium. The gelation pH had an effect in the crystalline phases formation. At pH 3 anatase was formed with traces of rutile while at pH 9 high extent of anatase phase is present.

The specific surface area was seven times larger in the samples calcined at 600°C compared with those calcined at 800°C, where a crystalline solid solution was formed, responsible of the large decrease in the specific surface area.

The catalytic activity was favored by the presence of BaO and Li_2O in the BaO-Li_2O-TiO_2-600°C sample as deduced from the low ignition temperature, high catalytic activity, in the ternary system compared with the TiO_2-Degussa.

Its large specific surface area, the anatase stability and its low crystallite size produced the high catalytic activity of the sample pH 9-600°C.

Acknowledgments

The authors thank CONACYT (Mexico) and CONICYT (Chile), Fondecyt 1020461 for their financial support, and Mr. A. Morales and Eng. M. Aguilar for technical support.

References

1. R. PRASSAD, L. KENNEDY and E. RUCKENSTEIN, *Catal. Rev. Sci. Eng.* **26** (1984) 1.
2. G. PECCHI, P. REYES, I. CONCHA and J. L. G. FIERRO, *J. Catal.* **179** (1998) 309.
3. R. B. ANDERSON, K. C. STEIN, J. J. FEENANA and L. E. J. HOFER, *Ind. Eng. Chem.* **53** (1961) 809.
4. P. REYES, A. FIGUEROA, G. PECCHI and J. L. G. FIERRO, *Catal. Today* **62** (2000) 209.
5. T. LÓPEZ, A. ROMERO and R. GÓMEZ, *J. Non-Cryst. Solids* **127** (1991) 105.
6. P. REYES, M. MORALES and G. PECCHI, *Bol. Soc. Chil. Quím.* **43** (1998) 391.
7. B. E. YOLDAS, *J. Mater. Sci.* **63** (1984) 145.
8. S. L. ANTONOVA and V. V. D'YAKOVA, *SOV. J. Glass Phys. Chem. (English Transl.)* **5** (1979) 607.
9. M. C. WEINBERG, G. F. NEILSON, G. L. SMITH, B. DUNN, G. S. MOORE and J. D. MACKENZIE, *J. Mater. Sci.* **20** (1985) 1501.
10. K. KAMIYA, S. SAKKA and Y. TATEMICHI, *ibid.* **15** (1980) 1765.
11. R. D. SHOUP and W. J. WEIN, U.S. Patent no. 4,059,658 (Nov. 22, 1977).
12. J. D. MACKENZIE and D. R. ULRICH, "Ultrastructure Processing of Advanvçced Ceramics" (Wiley, NY, 1988).
13. T. LÓPEZ, E. SÁNCHEZ, P. BOSCH, Y. MEAS and R. GÓMEZ, *Mater. Chem. Phys.* **32** (1992) 141.
14. J. S. WRIGHT and L. F. FRANCIS, *J. Mater. Res.* **8** (1993) 1712.
15. C. SUCKUT, R. A. HOWIE, A. R. WEST and L. M. TORREZ-MARTINEZ, *J. Mater. Chem.* **2** (1992) 1993.
16. C. F. BRINKER and G. W. SCHERER, "Sol-Gel Science. The Physics and Chemistry of Sol-Gel Processing" (Academic Press, 1990).
17. R. D.GONZÁLEZ, T. LÓPEZ and R. GÓMEZ, *Catal. Today* **35** (1997) 293.
18. J. RODRÍGUEZ-CARBAJAL, Laboratoire Leon Brillouin (CEA-CNRS), France Tel:(33)169083343, Fax:(33)16908 8261, E-mail: juan@llb.saclay.cea.fr
19. P. THOMPSON, D. E. COX and J. B. HASTING, *J. Appl. Crystallogr.* **20** (1987) 79.
20. R. A. YOUNG and P. DESAI, *Arch. Nauki Mat.* **10** (1989) 71.
21. E. PRINCE, *J. Appl. Crystallogr.* **14** (1981) 157.
22. P. P. LOTTICI, D. BERSANI, M. BRAGHINI and A. MONTENERO, *J. Mater. Sci.* **28** (1993) 177.
23. D. BERSANI, G. ANTONIOLI, P. P. LOTTICI and T. LÓPEZ, *J. Non-Cryst. Solids* **232** (1998) 175.
24. D. BERSANI, P. P. LOTTICI, T. LÓPEZ and X.-Z. DING, *J. Sol-Gel Sci. Tech.* **13** (1998) 849.
25. (a) T. LÓPEZ, R. GÓMEZ, G. PECCHI, P. REYES, X. BOKHIMI and O. NOVARO, *Mat. Lett.* **40** (1999) 59; (b) X. BOKHIMI, A. MORALES, O. NOVARO, T. LÓPEZ, E. SÁNCHEZ and R. GÓMEZ, *J. Mater. Res.* **10** (1995) 2788.
26. T. LÓPEZ, E. SÁNCHEZ, P. BOSCH, Y. MEAS and R. GÓMEZ, *Mater. Chem. Phys.* **32** (1992) 141.
27. BOKHIMI, A. MORALES, O. NOVARO, T. LÓPEZ, E. SÁNCHEZ and R. GÓMEZ, *J. Mater. Res.* **10** (1995) 2788.
28. C. DUSSARRAT, R. A. HOWIE, C. MATHER, L. M. TORRES-MARTÍNEZ and A. R. WEST, *J. Mater. Chem.* **95** (1991) 4059.

Received 8 October 2002
and accepted 16 September 2003